A Novel Nonlinear Super-twisting L 1 Adaptive Control for PKMs: From Design to Real-time Experiments

Youcef Mohamed Fitas, Ahmed Chemori, Johann Lamaury, Thierry Roux

HAL Id: lirmm-04577906

https://hal-lirmm.ccsd.cnrs.fr/lirmm-04577906v1

Submitted on 16 May 2024

A Novel Nonlinear Super-twisting $\mathscr{L}_1$ Adaptive Control for PKMs: From Design to Real-time Experiments

Youcef Fitas[1,2], Ahmed Chemori[1], Johann Lamaury[2] and Thierry Roux[2]

Abstract— This paper deals with robust-adaptive control of Parallel Kinematic Manipulators (PKMs), where a novel super-twisting $\mathscr{L}_1$ adaptive controller is proposed. The objective is to increase the robustness towards uncertainties as well as external disturbances of the standard $\mathscr{L}_1$ adaptive controller, by incorporating a robust super-twisting term. The proposed controller as well as the original $\mathscr{L}_1$ adaptive controller, are detailed for robot manipulators. Next, the experimental testbed is described, along with some implementation issues on FOEHN parallel robot. The proposed control scheme is compared with some existing literature controllers in two experimental scenarios, highlighting notable improvements in tracking performance reaching up to 75% with respect to the standard $\mathscr{L}_1$ adaptive controller.

I. INTRODUCTION

Parallel Kinematic Manipulators (PKMs) offer several advantages thanks to their architecture, compared to their serial counterparts [1], [2]. As a result, numerous research studies on PKMs have emerged during the last decades, covering various topics such as mechanism optimization [3], kinematic and dynamic modeling [4], trajectory planning [5], and control [6]. However, controlling PKMs has consistently been regarded as a challenging task within the control community due to their highly nonlinear dynamics, their large uncertainties, and their time-varying parameters. Consequently, to guarantee good tracking performance, these complex nonlinearities should be meticulously considered in the control scheme design [7]. Indeed, the literature features several control schemes designed and effectively applied to PKMs. Some of these control schemes, such as PID-based controllers [8], [9], are non-adaptive. These decentralized controllers are designed without considering knowledge about the robot's dynamic model, making them the most widely adopted schemes in the industrial world thanks to their simplicity. However, they may exhibit some performance issues in the presence of uncertainties or external disturbances. To improve the robustness of these controllers, incorporating robustness terms (like in the Robust Integral of the Sign of the Error-RISE) can be a potential candidate solution. The resulting controllers are known as RISE-based controllers [10].

For applications involving high velocities and accelerations, most non-adaptive decentralized controllers often exhibit significant degradation in the tracking performance.

To address this issue, such controllers can be enhanced by compensating for the robot's dynamics, leveraging the benefits of modeling and identification processes. Examples of such enhanced schemes include computed torque control [11], and augmented feedforward RISE feedback control [12]. Alternatively, the robot's dynamic model can be used to develop optimization-based control schemes, such as LQR (Linear Quadratic Regulator) [13], LQG (Linear Quadratic Gaussian) [14], and MPC (Model Predictive Control) [15]. In the case of NMPC (nonlinear MPC), the prediction model is nonlinear, which can result in a substantial computational burden. Sliding mode controllers are model-based control schemes known for their robustness against uncertainties and external disturbances, achieved through the application of a discontinuous control term [16], [17]. However, this term can lead to a chattering phenomenon, especially in the case of first-order sliding mode control. Non-adaptive model-based control schemes are highly dependent on the dynamic model and thereby require an accurate dynamic model with a good knowledge of the dynamic parameters. Consequently, they have limitations in certain industrial applications where the dynamic model is frequently time-varying or unknown [7].

To overcome those limitations, adaptive control schemes have been developed. The concept revolves around enhancing the controller's ability to adapt to changes in the system and its environment. One design way is to incorporate real-time estimation of dynamic parameters into the control scheme, thereby enabling adaptive compensation within a model-based framework [18], [19]. This approach results in the ability to compensate for uncertainties and time-varying dynamic parameters in real time. However, it is worth noting that implementing this control solution may require a substantial tuning time of the control parameters and may need also a significant computational burden. Adaptive control can also be achieved by making the feedback gains adaptive. In [20], the proposed controller combines a nominal feedforward term for model-based compensation with a RISE feedback control term featuring adaptive feedback gains. In [21], the controller gains are designed to be adaptive in order to enforce the behavior of the controlled robot to be as close as possible to a reference model. This approach is commonly referred to as Model Reference Adaptive Control (MRAC).

$\mathscr{L}_1$ Adaptive Control is recognized as an extension of MRAC, featuring the inclusion of a state predictor and the application of a low-pass filter to the control input [22]. The purpose of this filter is to guarantee a decoupling between robustness and adaptation. In contrast to MRAC scheme, the $\mathscr{L}_1$ adaptive control strategy places its emphasis on

Y. Fitas (e-mail: youcef-mohamed.fitas@lirmm.fr), and A. Chemori (e-mail: ahmed.chemori@lirmm.fr) are with LIRMM, University of Montpellier, CNRS, Montpellier, France.

Y. Fitas (e-mail: youcef.fitas@symetrie.fr), J. Lamaury (e-mail: johann;lamaury@symetrie.fr), and T. Roux (e-mail: thierry.roux@symetrie.fr) are with SYMETRIE, Nîmes, France.

ensuring the controller's feasibility by partially compensating for the uncertainties within the control channel bandwidth [23]. Furthermore, the incorporation of a projection operator ensures the boundedness of the estimated parameters. Besides, $\mathscr{L}_1$ adaptive control does not need a dynamic model of the system, making it particularly advantageous. Due to these benefits, it has acquired an increasing interest and has been successfully applied to a variety of uncertain nonlinear systems [24], [25]. However, the inclusion of the filter can introduce a delay in the controller's reactivity, potentially leading to a degradation in the tracking performance. Furthermore, $\mathscr{L}_1$ adaptive control may exhibit sensitivity to high-frequency disturbances. This sensitivity may need the incorporation of additional control terms to ensure robustness in such scenarios.

Super-twisting sliding mode control is known for its robustness towards uncertainties and external disturbances, as well as its ability to achieve finite-time convergence of tracking errors [17]. In this paper, the design of a novel non-model-based adaptive robust controller is proposed, by the augmentation of the $\mathscr{L}_1$ adaptive controller with a robust super-twisting term. The resulting controller should enhance the tracking performance compared to the standard $\mathscr{L}_1$ adaptive control, leading to an appropriate solution for uncertain nonlinear systems. As a validation, the proposed controller has been implemented and tested through real-time experiments on a 6-DOF parallel manipulator. A comparative study with respect to both the standard $\mathscr{L}_1$ adaptive and PID controllers has been conducted.

The rest of the paper is structured as follows. In Section II, a short background on $\mathscr{L}_1$ adaptive control along with the proposed control scheme are detailed. Section III provides the description and modeling of FOEHN parallel robot as a potential application testbed, with some implementation issues. Section IV presents and discusses the obtained real-time experimental results. Finally, in Section V, some concluding remarks are provided, along with a discussion of potential future research directions.

II. PROPOSED CONTROL SCHEME

In this section, a short background on $\mathscr{L}_1$ adaptive control, followed by the design of the proposed controller, are detailed.

A. Background on $\mathscr{L}_1$ Adaptive Control

In the robotic community, for an n-DOF robotic manipulator, $q_d \in \mathbb{R}^n$ represents the vector of the desired joint positions, while $q \in \mathbb{R}^n$ represents the vector of the measured joint positions. Typically, the desired joint trajectories can be obtained from the Cartesian desired trajectories by solving the inverse kinematics problem. The measured trajectories of the controlled robot should closely follow the desired trajectories, and thus, the control scheme is designed to minimize the tracking error. To achieve this objective, let us first define the combined tracking error as follows:

$$r = (\dot{q} - \dot{q}_d) + \lambda (q - q_d) \qquad (1)$$

where $\lambda \in \mathbb{R}^+$ is a control design parameter. The control input vector, denoted by Γ, can be designed as a combination of a fixed state-feedback term, and an adaptive control term as follows:

$$\Gamma = A_m r + \Gamma_{Ad} \qquad (2)$$

where $A_m \in \mathbb{R}^{n \times n}$ is a Hurwitz matrix characterizing the transient response of the system, and $\Gamma_{Ad} \in \mathbb{R}^n$ is the adaptive control term. The combined tracking error dynamics of a robotic manipulator, under the control law presented in (2) can be expressed as follows:

$$\dot{r} = A_m r + \Gamma_{Ad} - \eta(t, r, q), \quad r(0) = r_0 \qquad (3)$$

where $\eta(t, r, q) \in \mathbb{R}^n$ is a nonlinear function, representing the nonlinear dynamics of the system, including uncertainties, external disturbances, and non-modeled phenomena. In order to develop an appropriate $\mathscr{L}_1$ adaptive controller, it is essential to parameterize this function within specific assumptions that take into account the various types of uncertainties [26]. These uncertainties may include unknown constant parameters, uncertain input gain, and unmodeled actuator dynamics within the controlled system [24]. As in [23], where the truncated infinity norm of r is considered. The nonlinear function $\eta(t, r, q)$ can be parameterized as follows:

$$\eta(t, r, q) = \theta(t) \|r_\tau\|_{\mathscr{L}_\infty} + \sigma(t), \quad \forall t \in [0, \tau] \qquad (4)$$

where $\theta(t), \sigma(t) \in \mathbb{R}^n$ are differentiable functions, and $\|(.)_\tau\|_{\mathscr{L}_\infty}$ is the truncated $\mathscr{L}_\infty$-norm of $(.)$. To guarantee the asymptotic convergence of r to zero at a rate depending on the choice of A_m, it is essential that the adaptive control term Γ_{Ad} effectively cancel all the uncertainties and nonlinearities within the system defined by the function $\eta(t, r, q)$ [26]. Given the unknown nature of these uncertainties, the main objective of Γ_{Ad} is then to estimate and compensate for these nonlinearities. To achieve this goal, a state predictor of r is designed as follows:

$$\dot{\hat{r}} = A_m \hat{r} + \Gamma_{Ad} - \left(\hat{\theta}(t) \|r_\tau\|_{\mathscr{L}_\infty} + \hat{\sigma}(t) \right) \\ - K\tilde{r}(t), \quad \hat{r}(0) = r_0 \quad (5)$$

where $K \in \mathbb{R}^{n \times n}$ is a high-frequency noise rejector matrix gain [24], and $\tilde{r}(t) = \hat{r}(t) - r(t)$ is the prediction error. The estimation of $\theta(t)$ and $\sigma(t)$, respectively denoted by $\hat{\theta}(t)$ and $\hat{\sigma}(t)$, are obtained through the following adaptation laws:

$$\dot{\hat{\theta}}(t) = \xi Proj\left(\hat{\theta}(t), P\tilde{r}(t) \|r_\tau\|_{\mathscr{L}_\infty} \right), \quad \hat{\theta}(0) = \theta_0 \quad (6)$$

$$\dot{\hat{\sigma}}(t) = \xi Proj\left(\hat{\sigma}(t), P\tilde{r}(t) \right), \quad \hat{\sigma}(0) = \sigma_0 \qquad (7)$$

where $\xi \in \mathbb{R}^+$ is the adaptation gain, and $P \in \mathbb{R}^{n \times n}$ is the solution of the following static Lyapunov equation:

$$PA_m + A_m^T P + Q = 0 \qquad (8)$$

with $Q \in \mathbb{R}^{n \times n}$ is a diagonal positive-definite matrix. The projection operator $Proj(\theta, y)$ is defined as follows:

$$Proj(\theta, y) \triangleq \begin{cases} y & \text{if } f(\theta) < 0 \\ y & \text{if } f(\theta) \geq 0 \\ & \text{and } \nabla f^T y \leq 0 \\ y - \frac{\nabla f}{\|\nabla f\|} \left\langle \frac{\nabla f}{\|\nabla\| f}, y \right\rangle f(\theta) & \text{if } f(\theta) \geq 0 \\ & \text{and } \nabla f^T y > 0 \end{cases} \tag{9}$$

where $f : \mathbb{R}^n \to \mathbb{R}$ is a smooth convex function, defined in our case as:

$$f(\theta) = \frac{(1 + \varepsilon)\theta^T \theta - \theta_{max}{}^2}{\varepsilon \theta_{max}{}^2} \tag{10}$$

with θ_{max} being the imposed norm bound, and ε is the projection tolerance bound to be tuned. As the projection operator is used, the estimated parameters should remain within their admissible limits. To achieve this objective, two respective norm upper bounds are defined, θ_b for $\hat{\theta}(t)$, and σ_b for $\hat{\sigma}(t)$, thereby the conditions $\|\hat{\theta}(t)\| < \theta_b$, $\|\hat{\sigma}(t)\| < \sigma_b$ are always satisfied [24]. Finally, the adaptive control term Γ_{Ad} is the output in the time domain of $\Gamma_{Ad}(s)$, defined as follows:

$$\Gamma_{Ad}(s) = C(s)\hat{\eta}(s) \tag{11}$$

where $C(s)$ is a diagonal matrix of BIBO[1]-stable strictly proper transfer functions of the low-pass filter, and $\hat{\eta}(s)$ is the Laplace transformation of $\hat{\eta}(t)$, defined as follows:

$$\hat{\eta}(t) = \hat{\theta}(t)\|r_\tau\|_{\mathscr{L}_\infty} + \hat{\sigma}(t) \tag{12}$$

B. Proposed Controller: Super-twisting $\mathscr{L}_1$ Adaptive Control (ST-$\mathscr{L}_1$ Adaptive)

The $\mathscr{L}_1$ adaptive control scheme is designed to effectively compensate for uncertainties and nonlinearities, without the need for a dynamic model during the control design process [24]. It achieves this while maintaining a decoupling between robustness and adaptation. Also, its adaptive mechanism, coupled with the projection operator, ensures boundedness of the estimated parameters [23]. As a result, it can be a suitable control solution for PKMs, particularly where dynamic modeling is challenging, along with their applications characterized by frequently changing dynamics.

However, the introduction of a low-pass filter in the adaptive control law can introduce a time delay to the adaptation mechanism, potentially affecting the compensation of nonlinearities and uncertainties. Furthermore, the saturation of estimated parameters, with their unknown structure, may result in a reduced controller efficiency towards high-dynamic variations and high-frequency disturbances [24].

An extended $\mathscr{L}_1$ adaptive controller, designed for PKMs, may significantly enhance the tracking performance while reducing the impact of its drawbacks. To this end, our study proposes the incorporation of a robust super-twisting term into the $\mathscr{L}_1$ adaptive control scheme. The primary objective of this design is to take benefit from the super-twisting
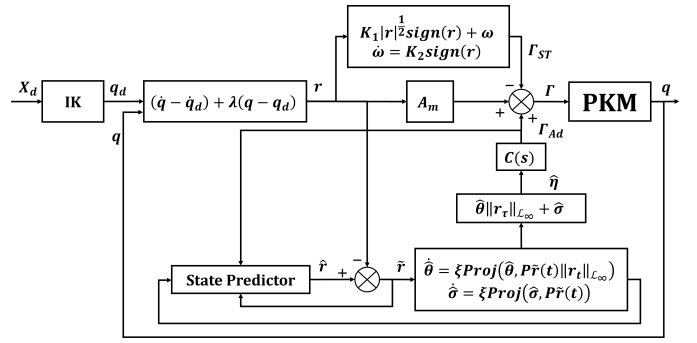
Fig. 1. Block diagram of the proposed control solution, ST-$\mathscr{L}_1$ Adaptive Controller.

algorithm advantages, which typically are not addressed by the conventional $\mathscr{L}_1$ adaptive controller [27]. The super-twisting algorithm is known for its robustness towards disturbances, particularly in the context of nonlinear systems [27]. Additionally, it has the capability to ensure finite-time convergence of both position and velocity tracking errors [27]. Furthermore, its adaptability to various types of system dynamics is a key feature, as it can be fine-tuned by adjusting its control parameters, according to specific characteristics of the PKM and its operating environment. To this end, the proposed controller in this paper combines $\mathscr{L}_1$ adaptive controller with a robust super-twisting term as follows:

$$\Gamma = A_m r + \Gamma_{Ad} - \left(K_1 |r|^{\frac{1}{2}} sign(r) + \omega \right) \tag{13}$$

$$\dot{\omega} = K_2 sign(r) \tag{14}$$

where $K_1, K_2 \in \mathbb{R}^{n \times n}$ are two positive definite diagonal matrices. The resulting control design can be effectively applied to PKMs, ensuring robustness against both uncertainties and external disturbances. The $\mathscr{L}_1$ adaptive control term serves to compensate for uncertainties and nonlinear dynamics, while the robust super-twisting term is incorporated to provide enhanced robustness. As a result, the proposed controller, which combines adaptive and robust feedback terms, should benefit from both $\mathscr{L}_1$ adaptive control and robust super-twisting algorithm advantages. This strategy should offer an improved performance in terms of adaptability and robustness against uncertainties as well as high-frequency disturbances, with enhanced tracking performance. Consequently, the proposed controller can be considered as a highly efficient combined adaptive-robust control solution for PKMs. To sum up, the block diagram of the proposed control scheme is depicted in Fig. 1.

III. ROBOT DESCRIPTION AND IMPLEMENTATION ISSUES

In this section, the experimental testbed is described, along with the parallel robot dynamic model, and some implementation issues.

A. Experimental Platform

FOEHN is a non-redundant Gough-Stewart platform manufactured by the company SYMETRIE. It's a 6-DOF parallel kinematic manipulator equipped with six independently

actuated legs powered by DC motors [2]. Its movement is controlled by adjusting the lengths of its legs, allowing precise manipulation of the moving platform. FOEHN has several advantages, including high accuracy, repeatability, and stiffness, making it a potential tool for a wide range of applications. These applications include motion simulations of vehicles, and naval and aeronautic systems. Also, this robot is particularly ideal for micro-positioning tasks [2]. FOEHN can carry payloads of up to $500\,kg$. The robot operational workspace includes translations of up to $\pm280\,mm$ and rotations of up to $\pm34.2°$. It can achieve maximum speeds of $500\,mm/s$ and $50°/s$, and maximum accelerations of $8600\,mm/s^2$ and $550°/s^2$, respectively.

FOEHN parallel robot is equipped with high-dynamic brushless DC motors and absolute EnDat 2.2 encoders. These motors can deliver a maximum torque of $18\,N.m$ and a maximum rotation speed of $3500\,rpm$. The encoders play a crucial role in the system, precisely measuring the angular positions of the motors (2^{20} counts per revolution) and facilitating the calculation of prismatic joint lengths. For control purposes, the motors are controlled by two multi-axis servo drives, each one is responsible for controlling three motors. The control torque inputs are transmitted to the drives from an OMRON CK3E controller, which operates at a servo cycle of $2\,kHz$ via an EtherCAT fieldbus. The servo control strategy is formulated in joint space, incorporating real-time calculated feedback on prismatic joint length. The applied controller is implemented using MATLAB/Simulink from MathWorks, and subsequently converted to the C language. Finally, the code is compiled and uploaded onto the CK3E controller. The desired trajectories are communicated to the CK3E controller via the SYM_Motion software, developed by SYMETRIE. This software serves as a Human-Machine Interface (HMI), enabling the creation, validation, and execution of multiple types of movements. It establishes seamless communication with the controller through a TCP/IP Ethernet connection.

B. Dynamic Model

The dynamic modeling of FOEHN parallel robot is conducted in both joint and moving platform spaces, using the Euler-Lagrange formulation. To simplify this dynamic model, the following assumptions have been considered:

- **Assumption 1**: Elastic phenomena are neglected, given the materials employed in the robot's design and fabrication, which exhibit minimal elastic effects.
- **Assumption 2**: The dry and viscous friction effects can be neglected in the passive universal joints, thanks to their optimal design.

Thanks to the differential kinematic model, and through its Jacobian matrix $J \in \mathbb{R}^{6\times6}$ [6], FOEHN's inverse dynamic model can be expressed in the joint space as follows:

$$M(q)\ddot{q} + C(q,\dot{q})\dot{q} + G(q) + \Gamma_f(\dot{q}) = \Gamma \qquad (15)$$

where $q, \dot{q}, \ddot{q} \in \mathbb{R}^6$ are vectors of the joint positions, velocities, and accelerations, respectively, $M(q) \in \mathbb{R}^{6\times6}$ is the robot total mass and inertia matrix, $C(q,\dot{q}) \in \mathbb{R}^{6\times6}$ is the Coriolis
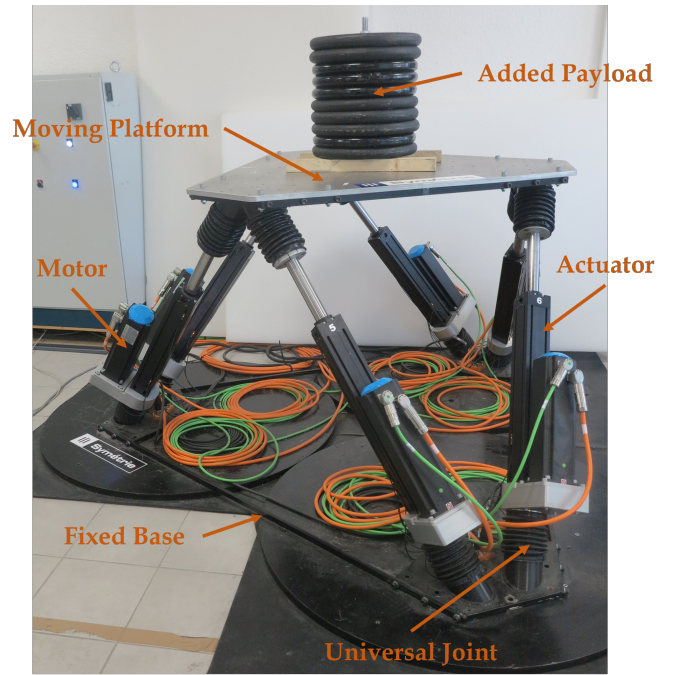

Fig. 2. Side view of experimental testbed (FOEHN parallel robot).

TABLE I

SUMMARY OF FOEHN ROBOT DYNAMIC PARAMETERS.

Parameter	Description	Value
m_p	Moving platform mass	$66\,Kg$
I_x	x axis moving platform inertia	$6.44\,kg.m^2$
I_y	y axis moving platform inertia	$6.44\,kg.m^2$
I_z	z axis moving platform inertia	$12.86\,kg.m^2$
I_m	Actuator inertia	$0.001018\,kg.m^2$
f_v	Viscous friction coefficient	$1.3283\,N.s/m$
f_s	Dry friction coefficient	$51.8714\,N$

and centrifugal forces matrix, $G(q) \in \mathbb{R}^6$ is the gravitational forces vector, $\Gamma_f(\dot{q}) \in \mathbb{R}^6$ is the friction vector, and $\Gamma \in \mathbb{R}^6$ is the vector of the control input torques. The dynamic parameters of FOEHN parallel robot are summarized in TABLE I. These parameters are determined through a series of distinct procedures. The mass of the moving platform was measured experimentally, while its inertia matrix was calculated using SolidWorks CAD software. Besides, the actuator inertia and friction coefficients were obtained through an experimental identification procedure [28].

C. Implementation Issues and Experimental Scenarios

To illustrate the effectiveness of the proposed ST-$\mathscr{L}_1$ Adaptive controller, a comparative study has been conducted, involving the standard $\mathscr{L}_1$ Adaptive controller [23], and a PID controller [8]. To facilitate this comparison, all three controllers are implemented on FOEHN parallel robot and tested under identical conditions. To this end, the following two experimental scenarios are considered:

- **Scenario 1 – nominal case:** Under nominal conditions, the three controllers are applied to the robot without the presence of uncertainties and external disturbances.
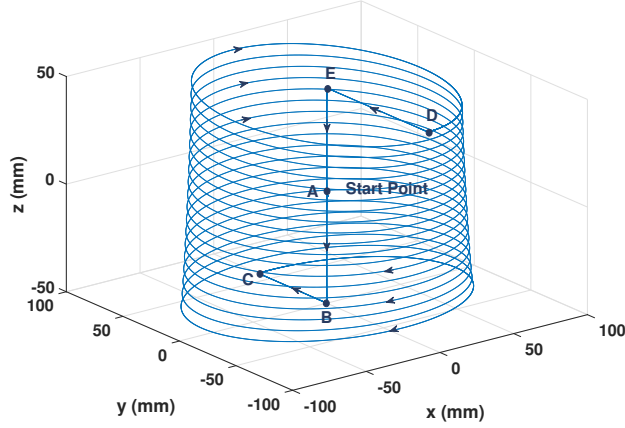
Fig. 3.   3D-view of the reference trajectory A-B-C-D-E-A.

involves systematically trying different sets of control gains in a real-time framework, and continuously adjusting them until the best control performance is achieved. The results of this tuning process for all controllers are summarized in TABLE II. It is worth noting that the estimated parameters for the adaptive controllers were initialized to zero.

IV. REAL-TIME EXPERIMENTAL RESULTS

In this section, the obtained real-time experiment results are presented and discussed for the two proposed experimental scenarios.

A. Scenario 1 – Nominal Case

The evolution of the joint tracking errors is depicted in Fig. 4. To accentuate the distinction between the controllers, the plot is zoomed in on the time interval between $10\,s$ and $12\,s$. Notably, the proposed control solution outperforms both the standard $\mathscr{L}_1$ adaptive and PID controllers, thanks to the incorporation of the super-twisting term alongside the non-model-based $\mathscr{L}_1$ adaptive control term. These improvements are further confirmed by the numerical calculation of the proposed evaluation metrics, as summarized in TABLE III. The evolution of the estimated parameters is depicted in Figs. 5 and 6. The incorporation of the projection operator ensures that these parameters remain within their admissible ranges. As a result of the proposed additional term, the estimated parameters for the proposed controller exhibit smaller amplitudes and mitigated oscillations. This outcome can be attributed to the compensation of certain dynamic effects and nonlinearities by the proposed super-twisting term. Consequently, a substantial difference between the adaptive terms of the original and the proposed controllers is evident.

The evolution of the generated control input torques is depicted in Fig. 7. To enhance the visual clarity, the plot has been zoomed in on the interval between $40\,s$ and $41\,s$. The generated torques remain within their admissible range, and the energy consumption is nearly identical for all the three controllers. However, it's worth mentioning that some overshoots are observed in the case of the $\mathscr{L}_1$ adaptive controller, primarily linked to the pronounced oscillations of the estimated parameters.

B. Scenario 2 – Robustness Towards Payload Changes

The joint tracking errors obtained with $200\,kg$ payload are displayed in Fig. 8. To better highlight the difference between the controllers, the plot is zoomed in within the range $[15\,s, 18\,s]$. Similar to the previous scenario, the proposed solution outperforms the other controllers, with a minor

- **Scenario 2 – robustness towards payload changes:** The controllers' robustness is tested by introducing an additional payload to the robot's moving platform. To this end, three distinct payloads, weighing respectively $100\,kg$, $150\,kg$, and $200\,kg$, were individually attached.

The reference desired trajectory for the moving platform translations is illustrated in Fig. 3. The platform starts motion with a point-to-point movement, traversing from A to B and subsequently to C (cf. illustration of Fig. 3). Next, it executes an elliptical trajectory from C to D. Finally, the moving platform mules from D to E, before returning to the starting point, A. For the rotational components, a sinusoidal trajectory is proposed, featuring an amplitude of $3°$ and a frequency of $0.3\,Hz$. A phase shift of $120°$ is maintained between the rotational angles (ϕ, θ, ψ). The whole duration of the reference trajectory is 50 seconds.

To quantify the tracking performance of the three controllers, the following RMS-based (Root Mean Square) criteria are proposed:

$$RMS_t = \sqrt{\frac{1}{N}\sum_{i=1}^{N}\left(e_x{}^2(i) + e_y{}^2(i) + e_z{}^2(i)\right)} \quad (16)$$

$$RMS_r = \sqrt{\frac{1}{N}\sum_{i=1}^{N}\left(e_\phi{}^2(i) + e_\theta{}^2(i) + e_\psi{}^2(i)\right)} \quad (17)$$

$$RMS_q = \sqrt{\frac{1}{N}\sum_{i=1}^{N}\left(\sum_{j=1}^{6} e_{q_j}^2(i)\right)} \quad (18)$$

where $e_x, e_y, e_z, e_\phi, e_\theta$, and e_ψ are the Cartesian tracking errors, $e_{q_j}, j = \overline{1,6}$ are the joint tracking errors, and N is the total number of samples.

The feedback gains of the three controllers have been experimentally tuned using a trial-and-error technique. For the proposed controller, the super-twisting gain was initially set to zero, and the tuning process began with the $\mathscr{L}_1$ adaptive control part. Subsequently, the gains of the super-twisting algorithm were tuned. The trial-and-error method
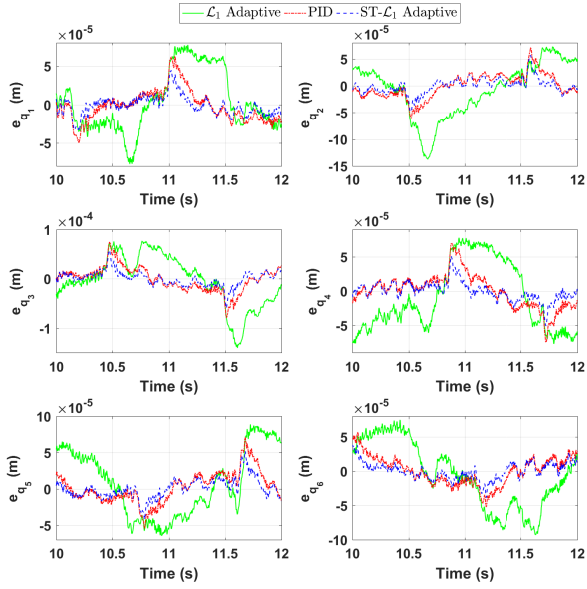
Fig. 4. Scenario 1: Evolution of joint tracking errors versus time.

Fig. 6. Scenario 1: Evolution of the estimated function $\hat{\sigma}(t)$ versus time.

Fig. 5. Scenario 1: Evolution of the estimated function $\hat{\theta}(t)$ versus time.
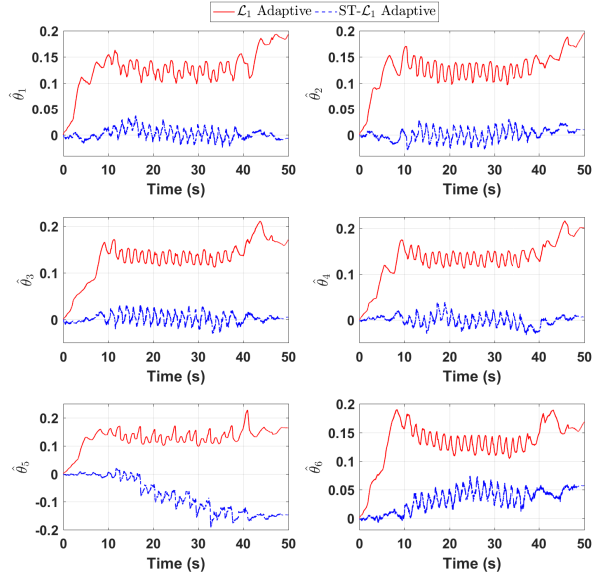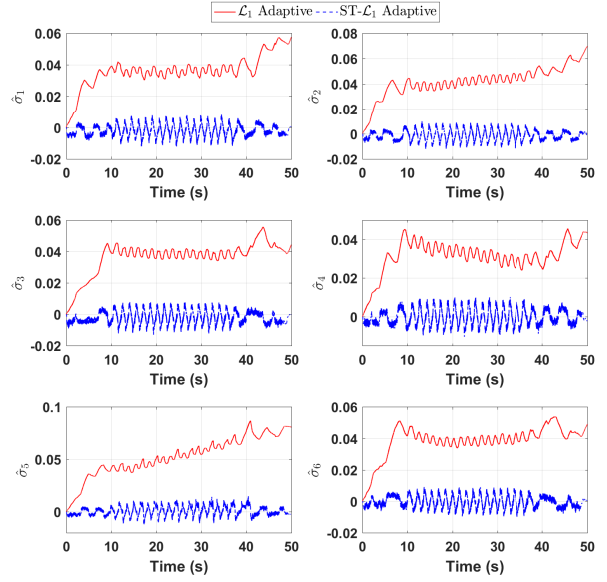

Fig. 7. Scenario 1: Evolution of input torques versus time.

TABLE III

SCENARIO 1: TRACKING PERFORMANCE EVALUATION WITH THE
ACHIEVED IMPROVEMENTS.

Controllers	$RMS_q(\mu m)$	$RMS_t(\mu m)$	$RMS_r(mdeg)$
$\mathcal{L}_1$ Adaptive	111.8656	92.2464	3.1772
PID	55.8083	46.8785	1.7687
ST-$\mathcal{L}_1$ Adaptive	35.0423	26.4935	1.4096
Imp./$\mathcal{L}_1$ Adaptive	68.67%	71.28%	55.63%
Imp./PID	37.21%	43.48%	20.30%

degradation compared to the nominal case. This demonstrates the capability of the proposed design to provide an enhanced control solution for PKMs, increasing the robustness against uncertainties and external disturbances. These improvements are further corroborated by the RMS values, summarized in TABLEs IV, V, and VI. The evolution of the estimated parameters is depicted in Figs. 9 and 10. As in the previous scenario, the inclusion of the projection operator ensures the boundedness of estimated parameters. In contrast to the original controller, the proposed solution does not exhibit high amplitudes with overshoots, where the adaptive control
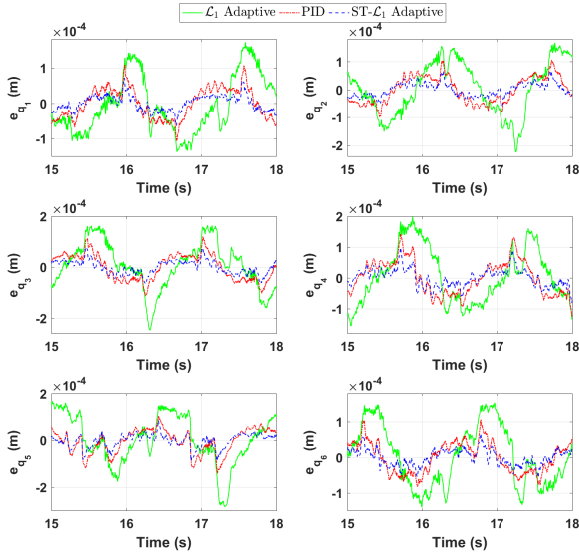
Fig. 8. Scenario 2 (200 kg payload): Evolution of joint tracking errors versus time.
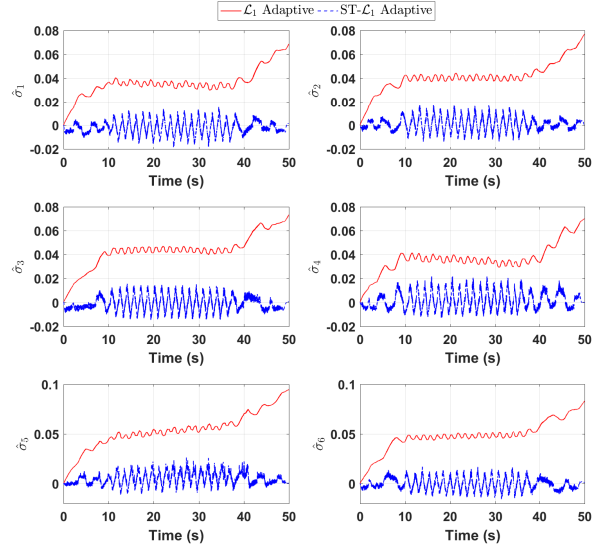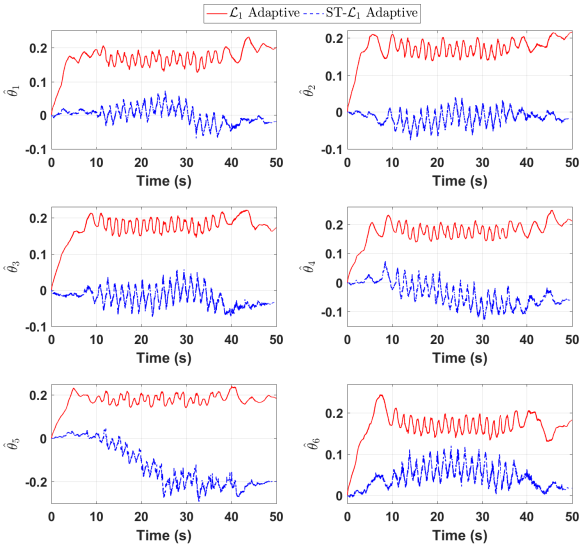

Fig. 9. Scenario 2 (200 kg payload): Evolution of the estimated function $\hat{\theta}(t)$ versus time.

Fig. 10. Scenario 2 (200 kg payload): Evolution of the estimated function $\hat{\sigma}(t)$ versus time.
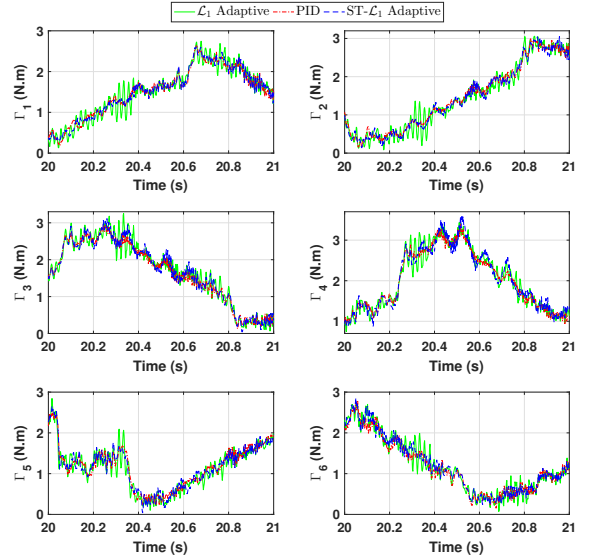

Fig. 11. Scenario 2 (200 kg payload): Evolution of input torques versus time.

term of the original controller compensates for all structured and unstructured uncertainties. The evolution of the control input torques is depicted in Fig. 11, and for better visibility, the plot has been zoomed in within the range $[20\,s, 21\,s]$. Notably, the generated torques remain within the admissible limits, and all controllers require almost the same quantity of energy.

V. CONCLUSION AND FUTURE WORK

In this paper, a novel super-twisting $\mathscr{L}_1$ adaptive controller is proposed to improve the tracking performance of PKMs,

TABLE IV

SCENARIO 2 (100 KG PAYLOAD): TRACKING PERFORMANCE
EVALUATION WITH THE ACHIEVED IMPROVEMENTS.

Controllers	$RMS_q(\mu m)$	$RMS_t(\mu m)$	$RMS_r(mdeg)$
$\mathscr{L}_1$ Adaptive	152.9350	124.4302	4.2197
PID	71.3322	60.1363	2.2515
ST-$\mathscr{L}_1$ Adaptive	42.7647	33.0331	1.6708
Imp./$\mathscr{L}_1$ Adaptive	72.03%	73.45%	60.40%
Imp./PID	40.05%	45.06%	25.79%

TABLE V

SCENARIO 2 (150 KG PAYLOAD): TRACKING PERFORMANCE
EVALUATION WITH THE ACHIEVED IMPROVEMENTS.

Controllers	$RMS_q(\mu m)$	$RMS_t(\mu m)$	$RMS_r(mdeg)$
$\mathscr{L}_1$ Adaptive	182.1214	146.9965	4.7940
PID	84.6723	72.3997	2.5423
ST-$\mathscr{L}_1$ Adaptive	47.2451	36.4234	1.8486
Imp./$\mathscr{L}_1$ Adaptive	74.05%	75.22%	61.43%
Imp./PID	44.20%	49.69%	27.28%

TABLE VI

SCENARIO 2 (200 KG PAYLOAD): TRACKING PERFORMANCE
EVALUATION WITH THE ACHIEVED IMPROVEMENTS.

Controllers	$RMS_q(\mu m)$	$RMS_t(\mu m)$	$RMS_r(mdeg)$
$\mathscr{L}_1$ Adaptive	197.6922	160.5205	4.9999
PID	91.4751	78.9590	2.6493
ST-$\mathscr{L}_1$ Adaptive	50.6191	39.7406	1.8921
Imp./$\mathscr{L}_1$ Adaptive	74.39%	75.24%	62.15%
Imp./PID	44.66%	49.67%	28.58%

especially in terms of robustness towards uncertainties and external disturbances. A short background on $\mathscr{L}_1$ adaptive control is introduced, along with the proposed contribution. Then, the experimental platform (FOEHN parallel robot) is presented with its dynamics and some implementation issues. The proposed controller has been experimentally validated and compared with the standard $\mathscr{L}_1$ adaptive controller as well as a PID controller in different operating conditions, demonstrating clear improvements in the tracking performance. In future work, the proposed control solution might be enhanced by designing a time-delay super-twisting algorithm. Additionally, its applicability extension to different platforms of PKMs can also be investigated, along with a thorough stability analysis of the resulting closed-loop system.

REFERENCES

[1] R.-M. A. Nzue, J.-F. Brethé, E. Vasselin, and D. Lefebvre, "Comparison of serial and parallel robot repeatability based on different performance criteria," *Mechanism and Machine Theory*, vol. 61, pp. 136–155, 2013.

[2] B. Dasgupta and T. Mruthyunjaya, "The stewart platform manipulator: a review," *Mechanism and Machine Theory*, vol. 35, no. 1, pp. 15–40, 2000.

[3] M. Wang, Y. Song, B. Lian, P. Wang, K. Chen, and T. Sun, "Dimensional parameters and structural topology integrated design method of a planar 5r parallel machining robot," *Mechanism and Machine Theory*, vol. 175, p. 104964, 2022.

[4] M. A. Khosravi and H. D. Taghirad, "Dynamic modeling and control of parallel robots with elastic cables: Singular perturbation approach," *IEEE Transactions on Robotics*, vol. 30, no. 3, pp. 694–704, 2014.

[5] E. Idà, T. Bruckmann, and M. Carricato, "Rest-to-rest trajectory planning for underactuated cable-driven parallel robots," *IEEE Transactions on Robotics*, vol. 35, no. 6, pp. 1338–1351, 2019.

[6] H. D. Taghirad, *Parallel robots: mechanics and control*. CRC press, 2013.

[7] W. Shang, F. Xie, B. Zhang, S. Cong, and Z. Li, "Adaptive cross-coupled control of cable-driven parallel robots with model uncertainties," *IEEE Robotics and Automation Letters*, vol. 5, no. 3, pp. 4110–4117, 2020.

[8] M. G. Villarreal-Cervantes and J. Alvarez-Gallegos, "Off-line pid control tuning for a planar parallel robot using de variants," *Expert Systems with Applications*, vol. 64, pp. 444–454, 2016.

[9] W. W. Shang, S. Cong, Z. X. Li, and S. L. Jiang, "Augmented nonlinear pd controller for a redundantly actuated parallel manipulator," *Advanced Robotics*, vol. 23, no. 12-13, pp. 1725–1742, 2009.

[10] H. Saied, A. Chemori, M. Bouri, M. El Rafei, C. Francis, and F. Pierrot, "A new time-varying feedback rise control for second-order nonlinear mimo systems: theory and experiments," *International Journal of Control*, vol. 94, no. 8, pp. 2304–2317, 2021.

[11] I. Davliakos and E. Papadopoulos, "Model-based control of a 6-dof electrohydraulic stewart–gough platform," *Mechanism and Machine Theory*, vol. 43, no. 11, pp. 1385–1400, 2008.

[12] J. M. Escorcia-Hernández, A. Chemori, H. Aguilar-Sierra, and J. Arturo Monroy-Anieva, "A new solution for machining with ra-pkms: Modelling, control and experiments," *Mechanism and Machine Theory*, vol. 150, p. 103864, 2020.

[13] Y. Yun and Y. Li, "Active vibration control based on a 3-dof dual compliant parallel robot using lqr algorithm," in *2009 IEEE/RSJ International Conference on Intelligent Robots and Systems*, pp. 775–780, IEEE, 2009.

[14] G. Chen, S. Hutchinson, and F. Dellaert, "Locally optimal estimation and control of cable driven parallel robots using time varying linear quadratic gaussian control," in *2022 IEEE/RSJ International Conference on Intelligent Robots and Systems (IROS)*, pp. 7367–7374, 2022.

[15] A. Chemori, R. Kouki, and F. Bouani, "A new fast nonlinear model predictive control of parallel manipulators: Design and experiments," *Control Engineering Practice*, vol. 130, no. 4, p. 1105367, 2023.

[16] Y. Fitas, A. Chemori, J. Lamaury, and F. Pierrot, "A new time-varying adaptive feedforward sliding mode control of pkms," *IFAC-PapersOnLine*, vol. 55, no. 12, pp. 621–626, 2022. 14th IFAC Workshop on Adaptive and Learning Control Systems ALCOS 2022.

[17] H. Saied, A. Chemori, M. Bouri, M. E. Rafei, and C. Francis, "Feedforward super-twisting sliding mode control for robotic manipulators: Application to pkms," *IEEE Transactions on Robotics*, pp. 1–18, 2023.

[18] W.-W. Shang, S. Cong, and Y. Ge, "Adaptive computed torque control for a parallel manipulator with redundant actuation," *Robotica*, vol. 30, no. 3, p. 457–466, 2012.

[19] M. R. J. Harandi, A. Hassani, M. I. Hosseini, and H. D. Taghirad, "Adaptive position feedback control of parallel robots in the presence of kinematics and dynamics uncertainties," *IEEE Transactions on Automation Science and Engineering*, pp. 1–11, 2023.

[20] M. Escorcia-Hernández, Jonatan, A. Chemori, and H. Aguilar-Sierra, "Adaptive rise feedback control for robotized machining with pkms: Design and real-time experiments," *IEEE Transactions on Control Systems Technology*, vol. 31, no. 1, pp. 39–54, 2023.

[21] M. Ghafarian Tamizi, A. A. Ahmadi Kashani, F. Abed Azad, A. Kalhor, and M. T. Masouleh, "Experimental study on a novel simultaneous control and identification of a 3-dof delta robot using model reference adaptive control," *European Journal of Control*, vol. 67, p. 100715, 2022.

[22] M. Bennehar, A. Chemori, F. Pierrot, and V. Creuze, "Extended model-based feedforward compensation in l1 adaptive control for mechanical manipulators: Design and experiments," *Frontiers in Robotics and AI*, vol. 2, pp. 1–11, 2015.

[23] M. Bennehar, A. Chemori, and F. Pierrot, "$\mathscr{L}_1$ adaptive control of parallel kinematic manipulators: Design and real-time experiments," in *2015 IEEE International Conference on Robotics and Automation (ICRA)*, pp. 1587–1592, IEEE, 2015.

[24] N. Hovakimyan and C. Cao, $\mathscr{L}_1$ *Adaptive Control Theory: Guaranteed Robustness with Fast Adaptation*. SIAM, 2010.

[25] D. Maalouf, V. Creuze, and A. Chemori, "A novel application of multivariable $\mathscr{L}_1$ adaptive control: From design to real-time implementation on an underwater vehicle," in *2012 IEEE/RSJ International Conference on Intelligent Robots and Systems*, pp. 76–81, 2012.

[26] K.-D. Nguyen, H. Dankowicz, and N. Hovakimyan, "Marginal stability in $\mathscr{L}_1$–adaptive control of manipulators," in *Proceedings of the 9th ASME International Conference on Multibody Systems, Nonlinear Dynamics, and Control*, vol. 7, 08 2013.

[27] Y. Shtessel, C. Edwards, L. Fridman, and A. Levant, *Sliding Mode Control and Observation (Control Engineering Series)*. Springer, 2014.

[28] W. Khalil and E. Dombre, "Modeling, identification and control of robots," *Applied Mechanics Reviews*, vol. 56, pp. B37–B38, 05 2003.